ISSN 1330-3651 (Print), ISSN 1848-6339 (Online)
Received: 7 June 2025; Accepted: 21 September 2025

https://doi.org/10.17559/TV-20250607002729
Original scientific paper

Experimental Study on the Aerodynamics of a Hybrid Dolphin Airfoil

Zorana Z. DANČUO*, Ivan A. KOSTIĆ, Olivera P. KOSTIĆ, Aleksandar Č. BENGIN, Goran S. VOROTOVIĆ

Abstract: This paper presents an experimental study of the aerodynamic characteristics of a new hybrid Dolphin airfoil, designated NA-DEL 2415. This airfoil is part of a novel family of seven hybrid Dolphin airfoils obtained through modification of the leading edge of the original Dolphin airfoils for the assumed standard roughness case. These hybrid airfoils have demonstrated improved aerodynamic characteristics compared with the NACA series and superior characteristics relative to Taposu's original Dolphin airfoils. Experiments presented in this paper were conducted in the subsonic wind tunnel of the University of Belgrade - Faculty of Mechanical Engineering. The NACA 2415, Dolphin 2415, and NA-DEL 2415 airfoils were tested under identical conditions, at the same Reynolds number, with free boundary layer transition. The experimental results confirmed the general NA-DEL aerodynamic advantages previously obtained by CFD investigations at a higher Reynolds number. The development and experimental investigation of the NA-DEL 2415 airfoil represents a novel contribution to the field, offering both scientific innovation and significant potential for operational application in general aviation and unmanned aerial vehicles.

Keywords: dolphin airfoil; general aviation; hybrid NA-DEL airfoil family; unmanned aerial vehicles; wind tunnel tests

1 INTRODUCTION

Nature uses its resources optimally and efficiently. Its mechanisms are aligned with the requirements of life with notable adaptability. Scientific disciplines concerned with the implementation of natural phenomena and mechanisms in technology are bionics and biomimetics [1]. Some pertinent bionic research on aquatic mammals, including whales and dolphins, is presented in the referenced paper.

One study utilised the shape of the head of the *Phocoenoides dalli* dolphin to improve the aerodynamics of the symmetrical NACA 0018 airfoil [2]. Researchers accomplished this by tangentially merging the shape of the dolphin's head with the NACA 0018 airfoil in the leading edge zone. As a result, three new airfoil shapes were developed. The study was grounded in the concept of biomimicry, drawing inspiration from the dolphin's head to achieve significant improvements and develop hybrid airfoils.

In a study [3], the NACA 2412 airfoil was tested, with a new design inspired by the shape of a porpoise. The leading edge of the NACA 2412 airfoil was modified to enhance aerodynamic efficiency at low subsonic speeds. Results demonstrated that the porpoise-inspired airfoil outperformed the original NACA 2412 airfoil in terms of aerodynamic efficiency at low speeds.

Experimental tests were conducted to investigate the influence of dolphin skin morphology on boundary layer control [4], using simulated dolphin skin. It was hypothesised that maintaining a laminar boundary layer along the dolphin's body, where rigid bodies would typically exhibit a turbulent boundary layer, reduces drag, primarily frictional drag. Additionally, bumps and protrusions were also investigated [5-8]. In research from Stanford University [5], a correlation between the structure of the skin of the porpoise *Phocoenaphocoena* and its effects on hydrodynamic parameters was examined. The skin behaves like an "anisotropic compliant wall". Based on the cross-section of the porpoise's dorsal fin, a 3D model was created, and subsequently used in CFD to calculate hydrodynamic parameters. Conversely, the influence of bumps implemented on the leading edge of airfoils on their aerodynamic performance was investigated in other studies [6, 7]. The addition of bumps to the leading edge, inspired by the humpback whale flipper, aims to improve aerodynamic efficiency and potentially reduce wing mass through passive boundary layer control. In a wind tunnel test [8], the aerodynamic performance of a humpback whale flipper model was examined. A model with tubercles and a sectional airfoil, NACA 0020, was tested for comparison. The results indicated significant improvements in aerodynamic parameters for the model with bumps on the leading edge compared to the baseline flat model. Several further studies have explored the application of bumps on aerodynamic surfaces [9-12]. Additionally, the wavy leading edge has been studied for its potential reduction of noise pollution generated by aerodynamic surfaces in the field of aeroacoustics [13].

Together with aerodynamic and hydrodynamic tests, biomimetic and bionic research on dolphins and their potential application in robotics is also important to highlight. Bioinspired dolphin-like robots are presented in several notable studies [14-16].

A new class of airfoils, referred to as Dolphin airfoils, was modelled using mathematical concepts drawing inspiration from the dolphin as an aquatic mammal [17, 18]. This newly developed mathematical model enables the creation of various types of the so-called Dolphin airfoils. Although these airfoils are not directly modelled on biological organisms, their shapes bear a close resemblance to a dolphin's body, placing them in the same category as those in the aforementioned studies.

This study provides specific solutions for the NACA, Dolphin, and NA-DEL 2415 airfoils, derived from both computational and experimental investigations, complementing a novel mathematical concept. The objective is to validate the hypothesis that modifying the broader leading edge domain of the original Dolphin 2415 can yield a novel airfoil with enhanced aerodynamic characteristics. Although the numerical analysis and the experimental tests were conducted under different Reynolds number conditions, both approaches consistently demonstrated a clear trend of improved aerodynamic performance for the newly developed NA-DEL 2415 airfoil.

2 PRIOR NUMERICAL ANALYSES

The RANS system of equations and the SST k-ω turbulence model were employed for all calculations using the commercial software ANSYS Fluent. At the more advanced design stages of the hybrid airfoil families presented in this paper, more complex approaches, such as those applied in [19], will be considered.

A structured C-mesh was generated encompassing a 2D control volume with a length and height of 25 m. All analysed airfoils had a unit chord length of 1 m. For viscosity, the three-coefficient Sutherland method was employed. The calculations simulated a "standard roughness" case with early boundary layer transition, ata Reynolds number of six million, a constant temperature of T = 288,15 K, and an operating pressure of p = 101325 Pa. A two-dimensional density-based model was employed. The study included the Full Multi-Grid method for solution initialisation and steering, aiming to optimise the Courant number. This computational approach has been previously utilised in the calculation of highly complex subsonic and supersonic flow patterns [20-22]. Following numerical calculations, a significant shortcoming of the original Dolphin airfoils was observed. Previous research [23, 24] presented key findings in which the original Dolphin airfoil, designated Dolphin 2415, was analysed. The Dolphin 2415 airfoil is a geometrical counterpart to the widely used NACA 2415 airfoil in general aviation. The Dolphin 2415 counterpart mirrors the design, considering maximum camber, thickness, and longitudinal positions.

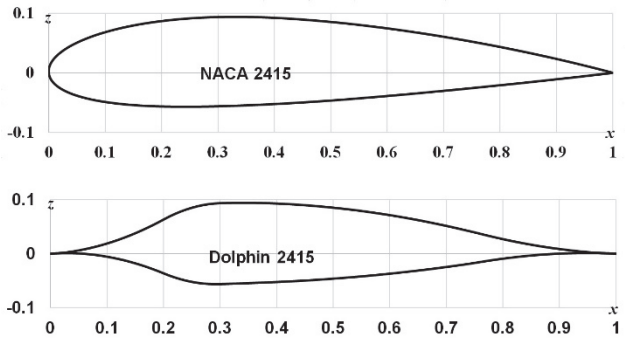

Figure 1 The NACA 2415 and Dolphin 2415 airfoils

Fig. 1 illustrates the geometry of the Dolphin airfoil with its unique sharp leading edge [17, 18]. At all angles of attack (AoA), the NACA 2415 airfoil maintained a smooth flow pattern around the leading edge. Its separation wake gradually propagated forward from the trailing edge with increasing AoA, up to stall at the critical AoA, α_{cr} = 14º. For Taposu's Dolphin 2415 airfoil, the separation bubble in the leading edge domain is apparent even at low AoA, such as α = 4°. At its stall angle (α_{cr} = 8°), noticeable zones of separated airflow both in the leading and the trailing edge domains are observed (Figs. 2 and 3). This results in a decline in overall aerodynamic performance. In comparison with the NACA2415 airfoil, the Dolphin 2415 exhibits a lower critical AoA, and a maximum lift coefficient reduced by 40,4%. The minimum drag coefficient is lower by 1,8%, and the maximum lift-to-drag ratio by 38,1%. The computational algorithm employed for these calculations was previously validated against experimental curves for the NACA 2415 from [25, 26] for the standard roughness case at MRe = 6,0.

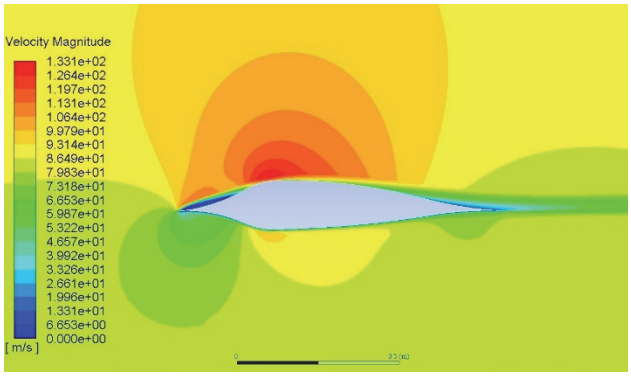

Figure 2 Velocity contours of the Dolphin 2415 airfoil at AoA α = 4°

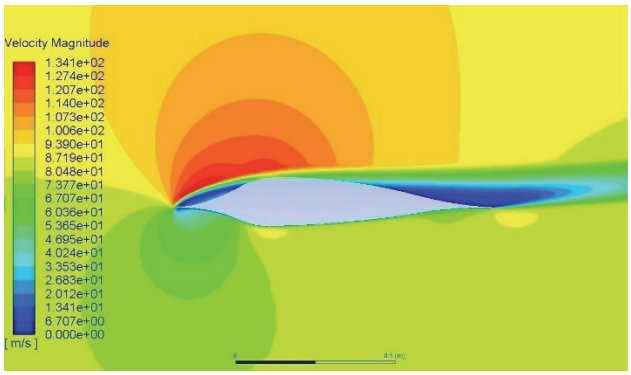

Figure 3 Velocity contours of the Dolphin 2415 airfoil at its critical AoA α_{cr} = 8°

3 THE NA-DEL MODIFICATION METHOD

The NA-DEL modification method was developed to enhance the hybrid airfoils obtained using the previously applied semi-elliptical method [26, 27]. It originated from the initial modification concept, the semi-elliptical "natural modification method" inspired by the velocity contours at specific AoAs and the flow field, resulting in a novel airfoil shape.

Following the semi-elliptical method, it was decided to adopt an alternative approach by connecting the NACA geometric counterparts with the corresponding original Dolphin airfoils at the maximum thickness domain. This was achieved by tangentially merging the front upper and lower surfaces of the NACA geometric counterpart up to the maximum thickness positions of the original Dolphin airfoil, which are located at the same distances from the leading edge on both airfoils. Taposu's original Dolphin airfoil was retained from these points to the trailing edge. The resulting hybrid airfoil was named the NA-DEL airfoil, derived from NA (NACA) and DEL ("Delfin" in Serbian, meaning Dolphin).

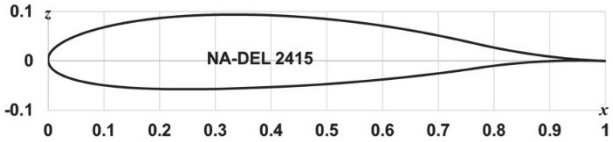

Figure 4 The NA-DEL 2415 airfoil geometry

To be precise, the original Dolphin 2415 airfoil was preserved from their shared maximum thickness coordinates - x = 0,34, z = 0,09403 on the upper camber,

and $x = 0{,}29$, $z = -0{,}05677$ on the lower camber-extending to the trailing edge. It was subsequently tangentially merged with the front domain of the NACA 2415 airfoil at the same positions, thereby forming the hybrid airfoil (Fig. 4). Numerical calculations were carried out under the same parameters as previously applied to both the NACA 2415 and the original Dolphin 2415 airfoils. Comparative results are presented in Tabs.1 and 2.

Table 1 Comparison of the lift, drag, and lift-to-drag ratio for the NACA 2415 airfoil

NACA 2415			
α / °	CL	CD	CL/CD
–6	–0,41	0,01135	–36,12
–4	–0,21	0,01008	–20,83
–2	–0,02	0,00953	–2,10
0	0,18	0,00962	18,71
2	0,38	0,01038	36,61
4	0,59	0,01183	49,87
6	0,79	0,01408	56,11
8	0,98	0,01727	56,75
10	1,14	0,02176	52,39
12	1,28	0,02838	45,10
14	1,36	0,03965	34,30
16	1,32	0,06288	20,99

Table 2 Comparison of the lift, drag, and lift-to-drag ratio for the NA-DEL 2415 airfoil

NA–DEL 2415			
α / °	CL	CD	CL/CD
–6	–0,51	0,01144	–44,58
–4	–0,27	0,00978	–27,61
–2	–0,03	0,00909	–3,30
0	0,21	0,00925	22,70
2	0,45	0,01020	44,12
4	0,69	0,01199	57,55
6	0,92	0,01477	62,29
8	1,14	0,01895	60,16
10	1,32	0,02566	51,44
12	1,43	0,03599	39,73
14	1,46	0,05194	28,11
16	1,41	0,07802	18,07

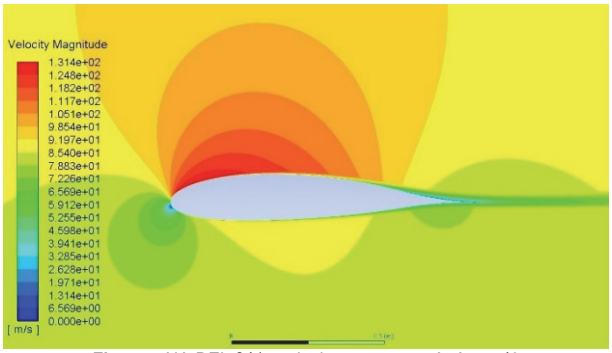

Figure 5 NA-DEL 2415 velocity contours at AoA α = 4°

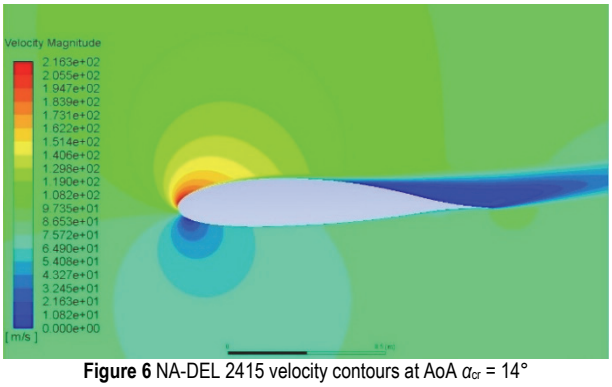

Figure 6 NA-DEL 2415 velocity contours at AoA α_{cr} = 14°

The critical AoA of the NA-DEL 2415 is 14°, representing a substantial improvement over the original Dolphin's AoA (with a critical AoA limited to 8º), thereby broadening the AoA range of practical applications. In comparison with the NACA 2415, the maximum lift coefficient of the NA-DEL 2415 airfoil exhibits an increase by 7,35%, alongside with an increase in the maximum lift-to-drag ratio by 9,76%. The minimum drag coefficient of the NA-DEL 2415 has been reduced by 4,62% [26]. This indicates that the NA-DEL 2415 airfoil has noticeably better aerodynamic characteristics than its predecessor, the original Dolphin 2415. The velocity contours (Figs. 5 and 6) illustrate the anticipated flow distribution, characterised by a smooth flow over the leading edge at all AoAs, which was clearly not the case for the original Dolphin (Figs. 2 and 3).

To evaluate the global aerodynamic characteristics of airfoils derived from the CFD analysis, the values corresponding to the NACA 2415 airfoil were adopted as the reference baseline, with its characteristic values formally normalised to 100%. These values were subsequently compared with the corresponding parameters of the Dolphin 2415 and NA-DEL 2415 airfoils (Tab. 3).

Table 3 Airfoil Comparison in Percentages / %

Airfoil	CLmax	CDmin	(CL/CD)max	Mean value / %
NACA2415	100	100	100	100
Dolphin 2415	59,55	98,21	61,88	74,40
NA-DEL 2415	107,25	95,38	109,76	107,21

To obtain the comparative average, the three values were summed and divided by three. If the resulting average exceeds 100%, the hybrid airfoil is deemed to be more aerodynamically efficient than the NACA variant. It is important to note that values below 100% for the minimum drag coefficient indicate an aerodynamic gain and confirm overall aerodynamic improvement.

To begin with, the percentage for the minimum drag coefficient is subtracted from 100. The resulting value is then added to 100. For example, the NA-DEL 2415 exhibits a minimum drag coefficient value of 95,38% (Tab. 3). When subtracted from 100, this yields 4,62%, which is subsequently added to 100%, resulting in a final value of 104,62%.

Next, this value is combined with the percentages for the maximum lift coefficient and the maximum lift-to-drag ratio of the NA-DEL 2415 airfoil (Tab. 3) and divided by three to calculate the average value, which in this case amounts to 107,21 %. Compared with the NACA 2415, the improvement demonstrated by the NA-DEL 2415 (Tab. 3, column 5) is evident. The practical engineering implications of the obtained numerical results clearly indicate that the NA-DEL 2415 airfoil is suitable for general aviation applications.

4 EXPERIMENT

4.1 General Descriptions

The experiments encompassed three airfoils within the 2415 category - the standard NACA 2415, the original Taposu Dolphin 2415, and the newly developed hybrid

NA-DEL 2415 airfoils. All models were constructed with a chord length of 0,4 m and a span of 0,8 m. To ensure two-dimensional flow conditions and to simulate an "infinite span" configuration, each airfoil model was mounted between two vertical boundary plates extending from the floor to the ceiling of the wind tunnel test section. The plates were positioned at a lateral distance of 0,804m. The two-millimetre gaps between the plates and the model were sealed using an elastic sponge-like duct tape affixed to the upper and lower model edges, ensuring tangential contact with the boundary plates. This arrangement prevented air leakage at the model boundaries, thereby enabling undisturbed force measurements and AoA adjustments (friction between the duct tape and boundary plates was negligible).

All tests were conducted in a closed-circuit subsonic wind tunnel at the Aerotechnical Institute, University of Belgrade - Faculty of Mechanical Engineering, Belgrade, Serbia. The conceptual 3D model for the three 2415 -type airfoil tests was developed using ANSYS Design Modeler (Fig. 7, [26]). AoA changes were performed via a manual kinematics system installed inside the test section. This process required either a near-complete power plant shutdown or operation in "idle" mode with flow speeds of 5 m/s between each new AoA measurement run (Fig.8, [26]). During facility setup and calibration, certain modifications and adjustments to the geometry had to be carried out on site.

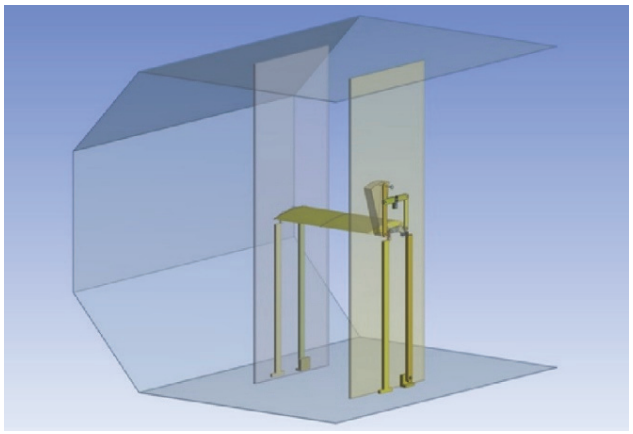

Figure 7 The 3D model of the experimental installation with an airfoil in the octagonal wind tunnel test section

Figure 8 The real-life manual system for AoA settings

The test installation was designed following the "yoke balance" concept [28], with its conceptual arrangement shown in Fig. 9. Measurements were carried out using five commercial force sensors: two, labelled as A_S and B_S for measuring the lift force, each with a maximum capacity of up to 10 kgf each (as originally specified in "kg" by the manufacturer). A further two, C_S and D_S, were used for measuring the drag force, while a fifth sensor, Es, was utilised to measure both the drag force and the pitching moment. These latter three sensors had a maximum capacity of up to 1 kgf. Preliminary calibration tests indicated that deliberately exceeding the sensors' rated capacity by 20% did not compromise their accuracy. Throughout all operational tests, the sensors' maximum range was never exceeded.

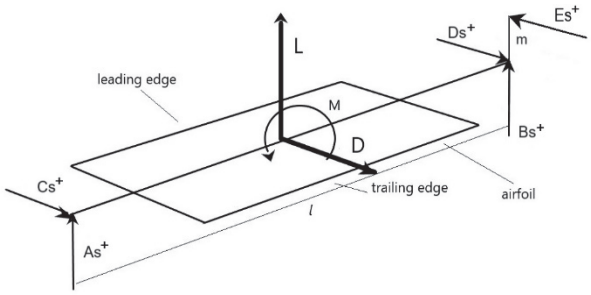

Figure 9 Sensors for lift, drag, and moment measurements with the adopted sign convention

From Eqs. (1) to (4) follows:

$$L = A_s + B_s \tag{1}$$

$$D = C_s + D_s - E_s \tag{2}$$

Pitching moment:

$$M = -E_s \times m \tag{3}$$

Additional condition, yawing moment:

$$-C_s + D_s - E_s\left(\frac{l}{2}\right) = 0 \tag{4}$$

The moment arm m was 0,2 m. The notations A_S, B_S, C_S, D_S, and E_S denote both the sensors and the respective forces recorded by them, with (+) indicating their assumed nominal positive directions, where Eq. (4) is supplementary [28], and was used for the additional validation of the values measured by these three sensors.

4.2 Measurements and Analyses of the Results

The testing process comprised three general phases. The first phase entailed the manufacturing, preparation, and detailed verification and adjustment of the test installation, including static calibration of the sensors and the entire measurement system without operating the wind tunnel power plant, as well as the construction of test models for the three airfoils. The second phase encompassed conducting the three series of wind tunnel runs, collecting raw sensor data, and converting it into forces and moments. The third and final phase involved post-processing and analysis of the collected data.

To ensure compatibility with the original gauge units, all static calibrations were performed using weights calibrated in kilograms. For fractional values, small plastic bottles filled with the appropriate amount of water were used as weights. Initially, each sensor was individually tested and validated on a test bench located outside the test section, and all sensors were found to be fully satisfactory.

Static calibrations of the complete measurement system were conducted separately: first by simulating the lift force using weights, then the drag force, and finally the pitching moment. The latter was simulated by applying a couple -equal forces in opposite vertical directions at the same moment arm - thereby avoiding the generation of additional lift. After each stage, several fine adjustments were made to both the measurement and load input systems. The procedure concluded with the simultaneous application of lift, drag, and pitching moment.

Following a series of modifications and the replacement of certain components and assemblies with improved versions, mutual interference between the measured components was reduced to a practically negligible level. For all three airfoils, two to three operational test runs were conducted within the same range of AoAs. The test results were averaged, without the need for further corrections due to interference. Fig. 10 presents the NACA 2415, Dolphin 2415, and NA-DEL 2415 airfoil models prepared for testing, and Fig. 11 shows the NA-DEL 2415 airfoil within the test section.

Following a series of modifications and the replacement of certain components and assemblies with improved versions, mutual interference between the measured components was reduced to a practically negligible level. For all three airfoils, two to three operational test runs were conducted within the same range of AoAs. The test results were averaged, without the need for further corrections due to interference. Fig. 10 presents the NACA 2415, Dolphin 2415, and NA-DEL 2415 airfoil models prepared for testing, and Fig. 11 shows the NA-DEL 2415 airfoil within the test section.

The temperatures in the tunnel test section ranged from 17 °C to 20 °C, and the ambient pressure varied between 994 and 1007 millibars. To ensure accurate data collection, measurements were taken at each AoA at speeds in closest proximity to the nominal 15 m/s. Pressure, temperature, and airspeed were recorded during each run, allowing for the calculation of air density. By measuring the exact airflow velocity achieved at a given AoA and the corresponding air density, it was possible to calculate the dynamic air pressure. These data were then used to derive the coefficients of lift, drag, and pitching moment from the forces measured by the five sensors (Fig. 9).

After each run, the power unit was stopped, and the force sensor measurement system was reset to zero. Although the flow velocity was a parameter set by the control unit, it varied by a few decimals in each run, likely due to the unavoidable slight fluctuations in the mains voltage. For each test, the dynamic viscosity was calculated using the Sutherland equation to determine the actual Reynolds number, which during these tests was approximately MRe = 0,4. (MRe = 0,3865 was the average across all runs). The experimentally obtained results for the aerodynamic coefficients are presented in Tabs. 4 to 6. Wall corrections were not applied at this stage, due to the primary aim of comparing the airfoils under the assumption that the wall effects were effectively the same in all three cases.

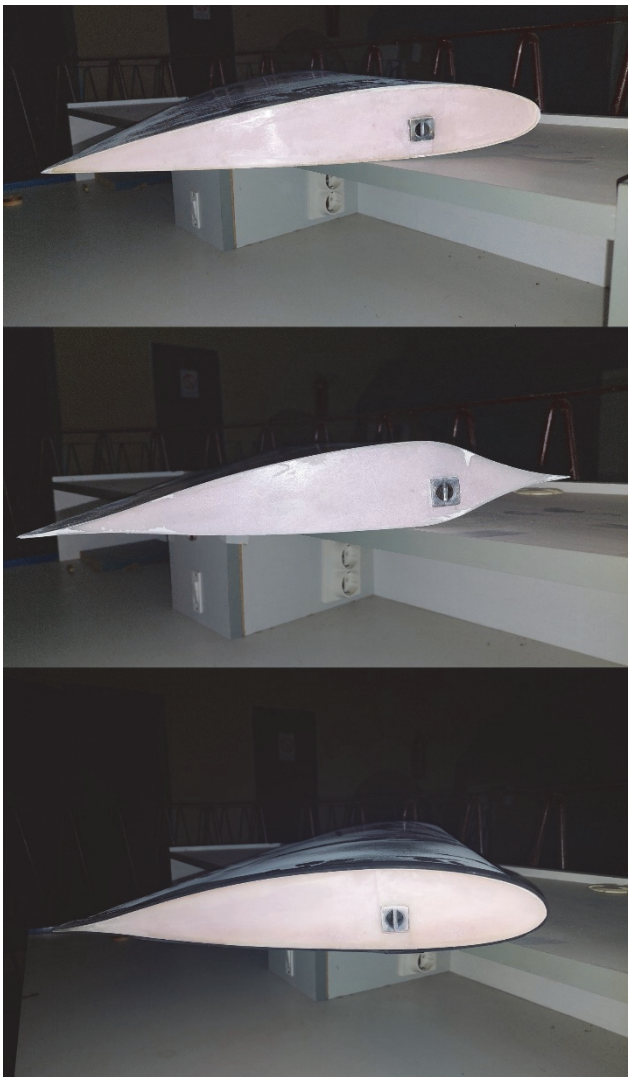

Figure10 Airfoil models NACA2415 (top), Dolphin 2415 (centre), and NA-DEL 2415 (bottom), used in wind tunnel tests, with AoA rotating axis located at 1/4 chord

Figure 11 The NA-DEL 2415 airfoil model used in wind tunnel experiments, mounted between boundary plates

For the NACA 2415 airfoil, measurements were conducted at airflow velocities ranging from 14,90 to 15,03 m/s, temperatures between 18,5 and 20,0 °C, and ambient pressures varying from 1004 to 1007 millibars.

Based on Tab. 4, the maximum experimental lift coefficient is 1,22, the minimum drag coefficient is 0,00540, and the maximum lift-to-drag ratio is 58,21.

For the original Dolphin 2415, measurements were conducted at airflow velocities ranging from 14,90 to 15,09 m/s, temperatures from 18,1 to 19,2 °C, and ambient pressures of 1007 mbar. As shown in Tab. 5, the maximum experimental lift coefficient is 0,993, the minimum experimental drag coefficient is 0,00418, and the maximum lift-to-drag ratio is 54,73.

Table 4 Averaged wind tunnel data for the NACA 2415 airfoil

α / °	CL	CD	Cm 1/4	(CL/CD)
–6	–0,36	0,01570	–0,0520	–22,93
–4	–0,18	0,00900	–0,0451	–20,00
–2	0,01	0,00560	–0,0434	1,79
0	0,20	**0,00540**	–0,0406	37,04
2	0,39	0,00670	–0,0379	**58,21**
4	0,59	0,01110	–0,0356	53,15
6	0,80	0,01830	–0,0408	43,72
8	0,95	0,02530	–0,0350	37,55
10	1,08	0,03420	–0,0228	31,58
12	1,17	0,04660	–0,0150	25,11
14	**1,22**	0,06790	–0,0150	17,97
16	1,20	0,09090	–0,0236	13,20
18	0,76	0,22500	–0,0870	3,38

Table 5 Averaged wind tunnel data for the original Dolphin 2415 airfoil

α / °	CL	CD	Cm 1/4	(CL/CD)
–6	–0,37	0,02701	–0,01644	–13,70
–4	–0,20	0,01440	–0,02148	–13.89
–2	–0,01	0,00724	–0,02346	–1,38
0	0,18	**0,00418**	–0,02778	43,06
2	0,37	0,00676	–0,03455	**54,73**
4	0,55	0,01567	–0,03734	35,10
6	0,69	0,02728	–0,03617	25,29
8	0,83	0,04537	–0,03636	18,29
10	0,93	0,06336	–0,03257	14,68
12	**0,993**	0,09512	–0,03716	10,44
14	0,991	0,14251	–0,06497	6,95
16	0,91	0,19210	–0,09059	4,74
18	0,77	0,22713	–0,09845	3,39

Table 6 Averaged wind tunnel data for the NA-DEL 2415 airfoil

α / °	CL	CD	Cm 1/4	(CL/CD)
–6	–0,40	0,01441	–0,03327	–27,76
–4	–0,18	0,00797	–0,03164	–22,58
–2	0,01	0,00473	–0,03190	2,11
0	0,22	**0,00362**	–0,03117	60,77
2	0,43	0,00588	–0,03043	**73,13**
4	0,64	0,01127	–0,02867	56,79
6	0,84	0,01754	–0,02706	47,89
8	1,01	0,02575	–0,02548	39,22
10	1,15	0,03739	–0,02280	30,76
12	1,22	0,05316	–0,02048	22,95
14	1,27	0,07366	–0,02296	17,24
16	**1,28**	0,10068	–0,02867	12,71
18	0,76	0,23082	–0,08934	3,29

Measurements for the NA-DEL 2415 airfoil were conducted at airflow velocities from14,83 to 15,06 m/s, temperatures from 17,0 to 18,1 °C, and ambient pressures ranging from 994 to 997 millibars. According to the values presented in Tab. 6, the maximum experimental lift coefficient is 1,28, the minimum experimental drag coefficient is 0,00362, and the maximum lift-to-drag ratio is 73,13.

Finally, Tab. 7 presents the relative differences in the maximum experimental lift coefficient, the minimum experimental drag coefficient, and the maximum experimental lift-to-drag ratio between the original Dolphin 2415 airfoil and the new hybrid NA-DEL 2415 airfoil, relative to the reference NACA 2415 airfoil.

Table 7 Relative change in lift coefficient, drag, and lift-to-drag ratio compared to the NACA 2415 airfoil

Airfoil	CLmax	CDmin	(CL/CD)max
NACA 2415	1,22	0,00540	58,21
Dolphin2415	0,993	0,00418	54,73
NA-DEL 2415	1,28	0,00362	73,13

Table 8 Relative changes in lift coefficient, drag coefficient, and lift-to-drag ratio compared to the NACA 2415 airfoil

Airfoil	Relative change / %	Relative change / %	Relative change / %
NACA 2415	/	/	/
Dolphin 2415	–18,60	–22,60	–5,97
NA-DEL 2415	+4,91	–32,96	+25,63

Based on the analysis of the experimental results presented in Tabs. 4 to 8, together with the graphs in Figs. 12-14, it can be concluded that the new hybrid NA-DEL 2415 airfoil exhibits better aerodynamic characteristics compared with both the Dolphin 2415 and the NACA 2415 airfoils. It achieves a higher maximum lift coefficient, a lower minimum drag coefficient, and a higher maximum lift-to-drag ratio across a broader range of AoAs. In the previous section, calculations were performed at an MRe value of 6,0, corresponding to the general aviation category and assuming standard surface roughness conditions. In contrast, the experiments were conducted at a significantly lower MRe value, on the order of 0,4, which corresponds to the fixed-wing UAV category, with natural boundary layer transition.

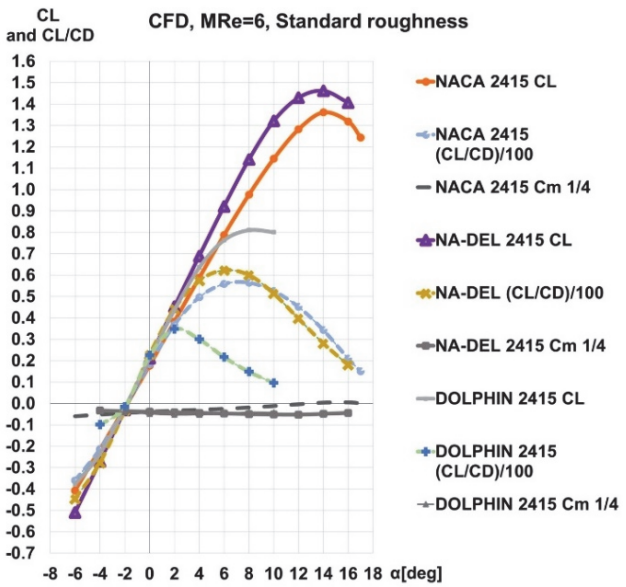

Figure 12 Lift, drag, lift-to-drag ratio, and pitching moment curves for the NACA 2415, Dolphin 2415 and NA-DEL 2415 airfoils obtained through CFD analyses

The overall conclusions regarding the advantages of the NA-DEL 2415 airfoil remain consistent, as illustrated in Figs. 12 to 15. As a result of the numerical and experimental investigations presented, the original plan to employ the new hybrid Dolphin airfoil NA-DEL 2415 in the general aviation category can be extended to smaller fixed-wing unmanned aerial vehicles.

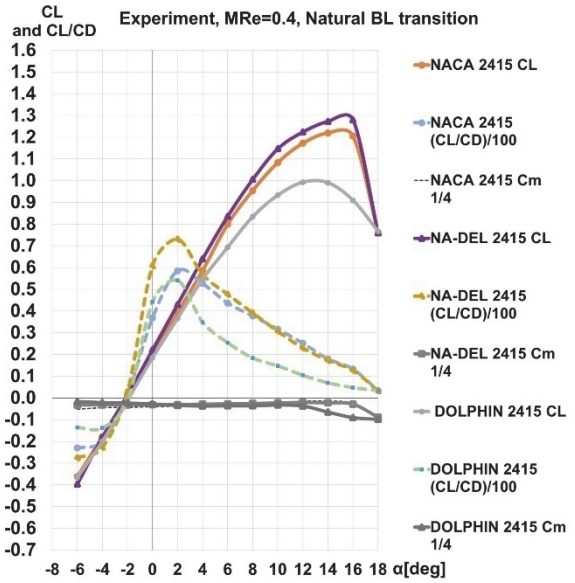

Figure 13 Experimental lift, drag, lift-to-drag ratio, and pitching moment curves for the NACA 2415, Dolphin 2415, and NA-DEL 2415 airfoils

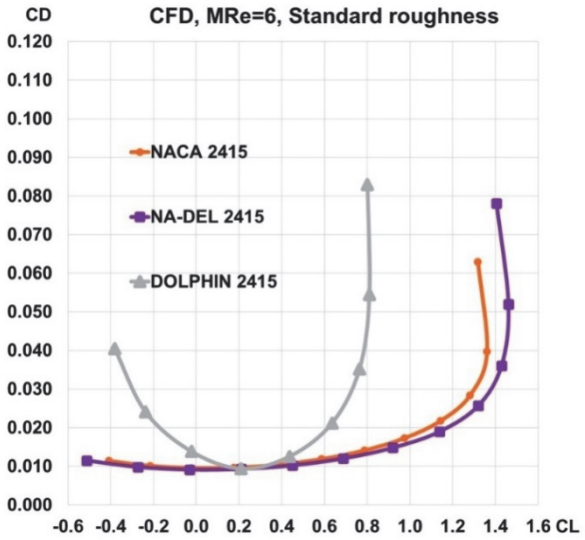

Figure 14CFD polar curves for the NACA 2415, Dolphin 2415, and NA-DEL 2415 airfoils under standard roughness conditions

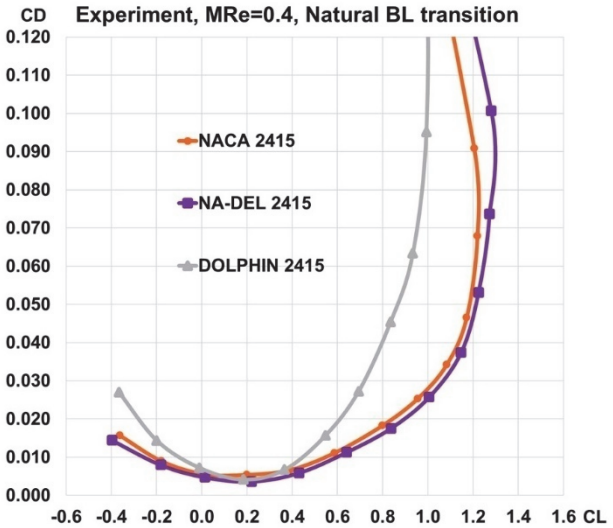

Figure 15 Experimental polar curves for the NACA 2415, Dolphin 2415, and NA-DEL 2415 airfoils under natural boundary layer transition conditions

4 CONCLUSION

The NA-DEL airfoil category presented in this paper has been developed based on a new geometrical principle. It entails merging the front domain of the corresponding NACA four-digit airfoil up to the point of maximum thickness with the remaining domain of the original Taposu's Dolphin airfoil counterpart, on both the upper and lower surfaces. Approximately 30% of the leading edge domain retains the geometry of the NACA, while the remaining 70% follows the geometry of the original Dolphin airfoil. This has yielded a "hybrid Dolphin" airfoil family, hereafter referred to as NA-DEL airfoils. The main contributions achieved through this approach are outlined below, presenting the results for 2415 geometry that has been analyzed both numerically and experimentally:

• All numerical calculations were performed using the commercial software ANSYS Fluent at a Reynolds number of million and the assumed standard roughness conditions, typically found on the lifting surfaces of general aviation aircraft. The computational model was initially validated through comparisons between the obtained numerical results for several NACA four-digit airfoils and the experimental data published in the renowned NACA Technical Report 824. Results obtained by CFD analysis indicate that, in comparison to its NACA 2415 counterpart, the NA-DEL 2415 airfoil exhibits a higher maximum lift coefficient and a lower minimum drag coefficient. Its maximum lift-to-drag ratio is also higher. Considering these three parameters, the advantages of the NA-DEL modification over the NACA airfoil are evident. Based on the averaging method introduced and explained in this paper, an overall improvement of +7,21% has been achieved (Tab. 3).

• CFD results have demonstrated that, compared with the original Taposu's Dolphin 2415 airfoil, the NA-DEL 2415 exhibits remarkably better aerodynamic characteristics. An average improvement of 32,81% has been recorded in favour of the NA-DEL configuration (Tab. 3). The velocity contours obtained from numerical simulations reveal a notably smooth flow pattern over the NA-DEL's leading edge up to the critical AoA, whereas the Dolphin displays a pronounced leading edge separation bubble even at low AoAs.

• Experimental investigations of the NA-DEL 2415 airfoil were conducted in the subsonic wind tunnel of the University of Belgrade - Faculty of Mechanical Engineering, Belgrade, Serbia, to verify the general conclusions about its advantages obtained from computational analysis. Due to limitations of the wind tunnel power plant, as well as budgetary constraints, all experiments were conducted at a lower Reynolds number of 400000, under natural boundary layer transition. Such flow conditions are typically representative of the small-to medium-sized fixed-wing UAVs.

• Wind tunnel tests were conducted using custom-built models of the NACA 2415, the original Dolphin 2415, and the NA-DEL 2415 airfoils. Most of the equipment used in the test section, including boundary plates, support structures with integrated force sensors, the AoA adjustment system, and so forth, was specifically designed and manufactured for these investigations.

• A system of five commercial strain-gauge sensors was employed to measure lift and drag forces, as well as the aerodynamic moment about the quarter-chord position. Prior to the actual testing, the measurement system was calibrated, statically tested using weights to simulate loads, and underwent several modifications and improvements in the pre-test verification phase. During the operational tests, in addition to force measurements, static pressure and temperature within the test section were also recorded and used to calculate air density and dynamic viscosity for each individual run.

• As these tests were primarily conducted for comparative purposes, no wind tunnel corrections have been applied thus far, and all presented results herein are "raw". The implementation of correction standard procedures is planned as part of the future work, within the context of more detailed investigations of the NA-DEL airfoil. It should also be noted that no CFD analyses were carried out in parallel with the experiments at a Reynolds number of 0,4 million. At such relatively low Reynolds numbers, ANSYS Fluent may produce results of questionable reliability; therefore, the focus at this stage was placed entirely on ensuring the accurate execution of the experiment.

• The experimental results confirmed that the NA-DEL 2415 airfoil also exhibits better aerodynamic performances compared with the NACA 2415 at MRe = 0,4. Using the NACA coefficient extremes as reference values, the NA-D EL achieved a maximum lift coefficient increase by 4,91%, a minimum drag coefficient decrease by 32,96%, and maximum lift-to-drag ratio increase by 25,63% (Tab. 8). At this Reynolds number, the original Dolphin airfoil exhibited all three parameters at lower values than the NACA, and considerably below the aerodynamic characteristics of NA-DEL airfoil.

Results from numerical calculations and experiments indicate that the NA-DEL 2415 airfoil can be effectively employed not only in general aviation design, but also in fixed-wing unmanned aerial vehicle applications. Further research will be undertaken to expand the NA-DEL hybrid airfoil family across a range of thickness ratios, maximum cambers and positions, through additional forthcoming computational and experimental investigations.

Acknowledgements

This research was supported by the Ministry of Science, Technological Development, and Innovation of the Republic of Serbia under contract number 451-03-136/2025-03/200213, dated February 4, 2025.

5 REFERENCES

[1] Iouguina, A., Dawson, J. W., Hallgrimsson, B., & Smart, G. (2014). Biologically informed disciplines: A comparative analysis of bionics, biomimetics, biomimicry, and bio-inspiration among others. *International Journal of Design & Nature and Ecodynamics*, *9*(3), 197-205. https://doi.org/10.2495/DNE-V9-N3-197-205

[2] Huang, S., Hu, Y., & Wang, Y. (2021). Research on aerodynamic performance of a novel dolphin head-shaped bionic airfoil. *Energy*, *214*, 118179. https://doi.org/10.1016/j.energy.2020.118179

[3] Raj Mohamed, M. A., Guven, U., & Yadav, R. (2019). Flow separation control of NACA-2412 airfoil with bio-inspired nose. *Aircraft Engineering and Aerospace Technology*, *91*(7), 1058-1066. https://doi.org/10.1108/AEAT-06-2018-0175

[4] Kramer, M. O. (1977). Boundary layer control by "artificial dolphin coating". *Naval Engineers Journal*, *89*(5), 41-45. https://doi.org/10.1111/j.1559-3584.1977.tb04243.x

[5] Pavlov, V. V. (2003). Wing design and morphology of the harbor porpoise dorsal fin. *Journal of Morphology*, *258*(3), 284-295. https://doi.org/10.1002/jmor.10135

[6] Hansen, K., Kelso, R., & Dally, B. (2009). The effect of leading edge tubercle geometry on the performance of different airfoils. *Proceedings of the ExHFT-7 Conference*.

[7] Hansen, K. L. (2012*). Effect of leading edge tubercles on airfoil performance*. Doctoral dissertation, University of Adelaide, School of Mechanical Engineering.

[8] Miklosovic, D. S., Murray, M. M., Howle, L. E., & Fish, F. E. (2004). Leading-edge tubercles delay stall on humpback whale (*Megaptera novaeangliae*) flippers. *Physics of Fluids*, *16*(5), 39-42. https://doi.org/10.1063/1.1688341

[9] Johari, H., Henoch, C., Custodio, D., &Levshin, A. (2007). Effects of leading-edge protuberances on airfoil performance. *AIAA Journal*, *45*(11), 2634-2642. https://doi.org/10.2514/1.28497

[10] Fish, F. E. & Battle, J. M. (1995). Hydrodynamic design of the humpback whale flipper. *Journal of Morphology*, *225*(1), 51-60. https://doi.org/10.1002/jmor.1052250105

[11] Stein, B. & Murray, M. M. (2005). Stall mechanism analysis of humpback whale flipper models. *Proceedings of Unmanned Untethered Submersible Technology (UUST)*, 5.

[12] Watts, P. & Fish, F. E. (2001). The influence of passive, leading edge tubercles on wing performance. *Proceedings of the Twelfth International Symposium of Unmanned Untethered Submersible Technology*, 2-9.

[13] Zhang, M. & Frendi, K. (2016). Bioinspired passive control of airfoil radiated noise. *22nd AIAA/CEAS Aeroacoustics Conference*, 2835. https://doi.org/10.2514/6.2016-2835

[14] Wang, Y., Yu, J., & Zhang, J. (2011). Modeling and simulation of porpoising for a multilink dolphin robot. In *2011 IEEE International Conference on Robotics and Biomimetics*, 2131-2136. https://doi.org/10.1109/ROBIO.2011.6181607

[15] Yu, J., Wu, Z., Su, Z., Wang, T., & Qi, S. (2019). Motion control strategies for a repetitive leaping robotic dolphin. *IEEE/ASME Transactions on Mechatronics*, *24*(3), 913-923. https://doi.org/10.1109/TMECH.2019.2908082

[16] Wu, Z., Liu, J., Yu, J., & Fang, H. (2017). Development of a novel robotic dolphin and its application to water quality monitoring. *IEEE/ASME Transactions on Mechatronics*, *22*(5), 2130-2140. https://doi.org/10.1109/TMECH.2017.2722009

[17] Țaposu, I. (1995). *Airfoil section* (Patent OSIM No. 11022171 995, European Patent No. 0772731/2002). Bucharest, Romania.

[18] Țaposu, I. (2002). *The Dolphin Profiles: A new concept in aerodynamics*. Bucharest, Romania: Editura Technica.

[19] Šekutkovski, B., Kostić, I., Stefanović, Z., Simonović, A., & Kostić, O. (2015). A hybrid RANS-LES method with compressible *k-ω* SST SAS turbulence model for high Reynolds number flow applications. *Tehnički Vjesnik*, *22*(5), 1237-1245. https://doi.org/10.17559/TV-20140404130058

[20] Kostić, O. P., Stefanović, Z. A., & Kostić, I. A. (2015). CFD modeling of supersonic airflow generated by 2D nozzle with and without an obstacle at the exit section. *FME Transactions*, *43*(2), 107-113. https://doi.org/10.5937/fmet1502107K

[21] Kostić, O. (2016). *Numerička simulacija strujnog polja vazduha u nadzvučnom mlazniku sa preprekom na izlazu* (*Computational simulation of air flow in supersonic nozzle with obstacle at exit, in Serbian*). Doctoral thesis, University

of Belgrade - Faculty of Mechanical Engineering, Belgrade, Serbia.
[22] Kostić, O., Stefanović, Z., & Kostić, I. (2017). Comparative CFD analyses of a 2D supersonic nozzle flow with jet tab and jet vane. *Tehnički Vjesnik*, *24*(5), 1335-1344. https://doi.org/10.17559/TV-20160208145336
[23] Dančuo, Z., Kostić, I., Kostić, O., Bengin, A., & Vorotović, G. (2022). Initial development of the hybrid semielliptical-dolphin airfoil. *Thermal Science*, *26*(3), 2199-2210. https://doi.org/10.2298/TSCI210515234D
[24] Dančuo, Z. Z., Kostić, I. A., Kostić, O. P., Bengin, A. Č., & Vorotović, G. S. (2022, September). Influence of thickness ratio on the aerodynamic characteristics of a family of hybrid semielliptical dolphin airfoils. *International Symposium on Aviation Technology, MRO, and Operations*, 1-7. https://doi.org/10.1007/978-3-031-42041-2_1
[25] Abbott, I. H., Von Doenhoff, A. E., & Stivers, L., Jr. (1945). *Summary of airfoil data* (No. NACA-TR-824). National Advisory Committee for Aeronautics.
[26] Dančuo, Z. Z. (2023a). *Razvoj familije hibridnih delfina aeroprofila* (*Development of a family of hybrid dolphin airfoils, in Serbian*). Doctoral thesis, University of Belgrade - Faculty of Mechanical Engineering, Belgrade, Serbia.
[27] Dančuo, Z. Z., Kostić, I. A., Kostić, O. P., Bengin, A. Č., & Vorotović, G. S. (2023b). Leading edge shape optimization of a novel family of hybrid dolphin airfoils. *Proceedings of the 9th International Congress of the Serbian Society of*, 35-45.
[28] Pope, A. & Harper, J. J. (1966). *Low-speed wind tunnel testing*. New York, NY: John Wiley & Sons.

Contact information:

Zorana Z. DANČUO, PhD, Research Associate
(Corresponding author)
University of Belgrade,
Innovation Center of the Faculty of Mechanical Engineering in Belgrade,
Kraljice Marije 16, 11000, Serbia
E-mail: zdancuo@mas.bg.ac.rs

Ivan A. KOSTIĆ, PhD, Full Professor
University of Belgrade, Faculty of Mechanical Engineering,
Kraljice Marije 16, 11000, Serbia
E-mail: ikostic@mas.bg.ac.rs

Olivera P. KOSTIĆ, PhD, Associate Professor
University of Belgrade, Faculty of Mechanical Engineering,
Kraljice Marije 16, 11000, Serbia
E-mail: okostic@mas.bg.ac.rs

Aleksandar Č. BENGIN, PhD, Full Professor
University of Belgrade, Faculty of Mechanical Engineering,
Kraljice Marije 16, 11000, Serbia
E-mail: abengin@mas.bg.ac.rs

Goran S. VOROTOVIĆ, PhD, Associate Professor
University of Belgrade, Faculty of Mechanical Engineering,
Kraljice Marije 16, 11000, Serbia
E-mail: gvorotovic@mas.bg.ac.rs